PHOTONICS Research

# Ultra-wide varifocal imaging with selectable region of interest capacity using Alvarez lenses actuated by a dielectric elastomer

Qun Hao,[1,2] Chuanxun Chen,[1] Jie Cao,[1,2] Zhikuo Li,[1] and Yang Cheng[1,2,*]

[1]Key Laboratory of Biomimetic Robots and Systems, Ministry of Education, Beijing Institute of Technology, Beijing 100081, China
[2]Yangtze Delta Region Academy of Beijing Institute of Technology, Jiaxing 314003, China
*Corresponding author: yangcheng2007@163.com

Received 31 January 2022; revised 2 May 2022; accepted 9 May 2022; posted 9 May 2022 (Doc. ID 455331); published 10 June 2022

**A remarkable feature of Alvarez lenses is that a wide focal length tuning range can be achieved using lateral displacement rather than commonly used axial translation, thus, reducing the overall length of varifocal imaging systems. Here, we present novel lens elements based on Alvarez lenses actuated by a dielectric elastomer (DE). The proposed lens elements are composed of the varifocal component and the scanning component. Based on the proposed lens elements, an imaging system is built to realize ultra-wide varifocal imaging with a selectable region of interest. The lens elements have a variable focus function based on an Alvarez lens structure and a DE actuator and a scanning function based on the DE-based four-quadrant actuators. The large deformation generated by the DE actuators permits the lateral displacement of the Alvarez lenses up to 1.145 mm. The focal length variation of the proposed varifocal component is up to 30.5 times, where the maximum focal length is 181 mm and the minimum focal length is 5.94 mm. The rise and fall times of the varifocal component are 160 ms and 295 ms, respectively. By applying different voltages on four-quadrant actuators, the scanning component allows the varifocal component to move in different directions and endows the varifocal component with a selectable region of interest imaging capability. The scanning range of the scanning component is 17.57°. The imaging resolution of the imaging system is approximately 181 lp/mm. The system developed in the current study has the potential to be used in consumer electronics, endoscopy, and microscopy in the future.** 

https://doi.org/10.1364/PRJ.455331

## 1. INTRODUCTION

Varifocal imaging is an essential function in many optics applications, such as biomedicine, photography, smartphones, and virtual reality [1–3]. Most demonstrated optical devices to date adopt mechanical axial movement of several lenses over specific distances along the optical axis to realize the varifocal function, which has many problems such as having a large volume, being expensive, showing mechanical wear, and being slow [4,5]. These devices left much to be the miniaturization modern optical imaging desired. To meet the demand for miniaturization, considerable efforts have been made to develop compact varifocal lenses. Adaptive lenses provide a more compact, faster response speed, and lighter-weight alternative than traditional varifocal lens assemblies [6,7]. According to the difference in operation mechanisms, adaptive lenses can be broadly classified into two categories: liquid lenses and liquid crystal lenses. The liquid lenses change the focal length by changing the curvature radius of the refractive surface [8]. Although many miniaturized liquid lenses have been proposed, including the membrane-less [9–11] and membrane-structured liquid lenses [12,13], these lenses suffer from some problems due to the intrinsic characteristics of the liquid, such as being sensitive to temperature and gravity, leaking easily, and having an unstable optical axis [14–17]. Liquid crystal lenses are subject to a graded refractive index distribution by changing the orientations of the directors under the application of an inhomogeneous electric field, thereby controlling the focal length [18,19]. However, there are some inherent limitations of the liquid crystal lenses, such as polarization dependence, small aperture, and unavoidable electrode inclusion on the optical path [20]. Besides liquid lenses and liquid crystal lenses, some other means can also be used to realize varifocal functionality [21–23].

Alvarez lenses, independently developed by Alvarez [24] and Lohmann [25] a few decades ago, are different types of lenses with varifocal capability. They are composed of a pair of lens elements, which have complementary cubic surface profiles. The Alvarez lenses provide a wide optical power tuning range through small lateral displacements perpendicular to the optical

axis, rather than the mechanical movement along the optical axis that is employed in the traditional varifocal lenses. Thus, the Alvarez lenses have the potential to achieve a more compact structure, a wider varifocal range, a faster response time, more ease of packaging, and higher stability, which can be a powerful alternative for miniature imaging systems [26]. Moreover, due to no liquid involved, the Alvarez lenses show several remarkable advantages in terms of temperature sensitivity, response speed, and environmental stability. When the two lens elements of the Alvarez lenses are aligned in registration, the resulting phase profile is null, and the Alvarez lenses do not focus light, which can be interpreted as having an infinite focal length. When the lens elements have a lateral movement, one with respect to the other, perpendicular to the optical axis, it allows the Alvarez lenses to change from a negative power lens to a positive power lens depending on the lateral movement direction [27–29].

Although the Alvarez lenses concept has been proposed for many years, it has not been widely used for a long time mainly due to fabrication challenges of the required cubic freeform surface [30]. Fortunately, benefiting from the advanced optical manufacturing technology, many optical systems using Alvarez lenses have also been studied [31,32]. The emerging diamond micromachining technology enables the manufacturing of the required surfaces of the Alvarez lenses with adequate depth modulation and surface finish. However, actuating the Alvarez lens with a large lateral movement in a simple method is a concern for the varifocal lenses based on the Alvarez lenses. The focal length variability of the Alvarez lenses has been realized by MEMS-driven technology [33]. The lateral displacement range of the micro-electromechanical systems (MEMS)-driven technology is usually less than 500 μm. A wide range of focal length tuning is difficult to achieve due to the small lateral displacement. Although some amplifiers can be used to enlarge lateral displacement, the size of the amplifier equipment is relatively large. A method of manually actuating the lateral movement of the Alvarez lenses is proposed [34,35], but the tuning speed and precision of the focal length cannot be scaled to the modern varifocal applications. Therefore, it is necessary to propose a novel driving mechanism of the Alvarez lenses in order to overcome the disadvantages of traditional actuation methods, including small displacement, slow speed, and complex structure. Moreover, when the interest region does not lie in the center of the field of view, it is necessary to align the central field of view with the region of interest because of the observation habit of the human eye and the high imaging quality in the central field of view for imaging systems [36]. The traditional method is to move the imaging target or to manually adjust the lens to make the region of interest located in the center of the field of view, which has the problems of low accuracy, slow response speed, and low efficiency [37].

To actuate the Alvarez lenses with a large displacement and high speed in a simple method, we present novel lens elements based on the Alvarez lenses actuated by dielectric elastomer (DE). The lens elements are composed of the varifocal component and the scanning component. The lens elements have a variable focus function based on the Alvarez lens structure and DE actuator and a scanning function based on the DE-based four-quadrant actuators. The proposed lens elements are used to develop an ultra-wide varifocal imaging system with selectable region of interest capability [38]. In particular, we show that the imaging system with such properties can be obtained by combining an emerging class of "artificial muscle" materials with the varifocal technology of Alvarez lenses.

## 2. DESIGN AND FABRICATION

The proposed lens elements comprise a varifocal component and a scanning component. The varifocal component is placed and fixed at the center of the scanning component, as shown in Fig. 1(a). The image of the fabricated lens elements is shown in Fig. 1(b). The varifocal component and scanning component are both driven by DE actuators. Within the family of electroactive polymers, DEs are quickly emerging as a top choice of "smart" materials for new kinds of soft actuators capable of high strain, high energy density, high efficiency, fast response speed, noise-free operation, high resilience, and lightweight [39]. When the driving voltage is applied to the DE membrane, the thickness of the DE decreases, and the surface increases under Maxwell stress [40].

The proposed varifocal component is mainly constructed from four acrylic frames, two lens elements of the Alvarez lenses, and two DE membranes. The two DE membranes are coated with compliant electrodes on local areas along both the left and right sides of the Alvarez lenses. The Alvarez lenses consist of two lens elements, where each lens element has a plane-freeform structure, i.e., one plane surface side and one free-form surface side described by a cubic polynomial equation, which can be given by [24,25,41]

$$t = A(xy^2 + x^3/3) + Dx + E, \tag{1}$$

where $A$, $D$, and $E$ are constants to be determined, $x$, $y$ are transverse coordinates normal to the $z$-direction, and $t$ is the phase profiles of the Alvarez lens. An amplitude coefficient $A$ controls the amount of free-form surface depth modulation over a given area. The constant $D$ defines the tilt of the free-form surface and can be used to reduce the overall thickness of the lens element. The constant $E$ is the bulk element thickness added to the cubic surface equation at the center. The two lens elements are mounted on the bottom surface and top surface of two DE membranes, respectively, and then are assembled to form the varifocal component based on the Alvarez lenses.

Initially, the two lens elements are precisely aligned along the optic axis and the cubic surfaces are inverted concerning each other. When there is no driving voltage applied to the compliant electrodes, the two lens elements act as a plate of constant thickness and thus have an infinite focal length (ignoring the air gap), as depicted in Fig. 1(c). When the driving voltage applied to the compliant electrodes is on, the electrostatic attraction of the DE membrane produces radially compressive force directing towards the lens at the center and subsequently pulls the lens elements to move relatively. The relative lateral movements of the two lens elements make the focal length of the varifocal component change, as shown in Fig. 1(d). The varifocal component acts as a convex lens when the first lens element moves in the negative $x$-direction as well as when the second lens element moves in the positive $x$-direction.

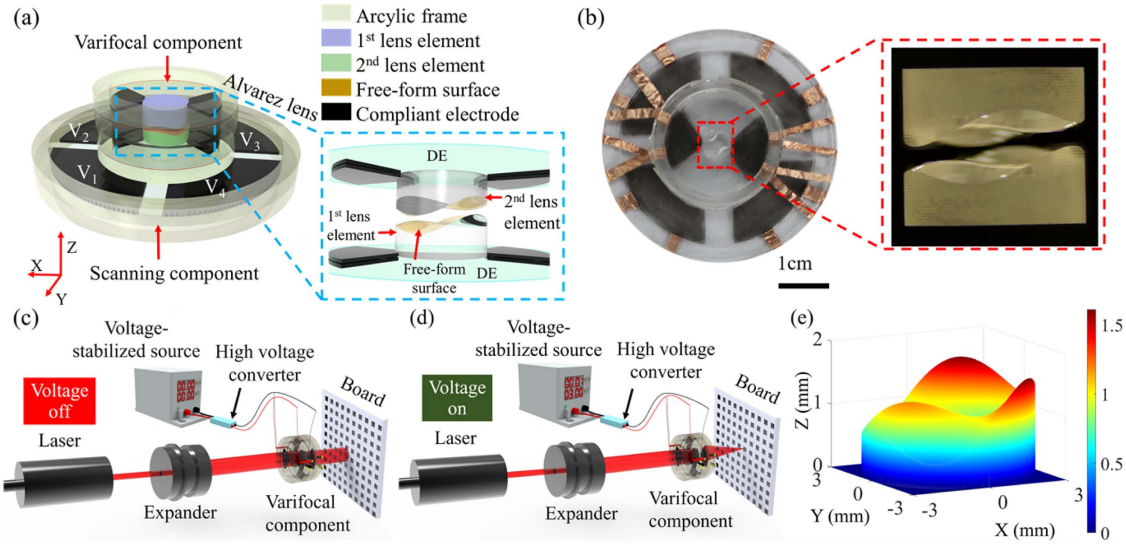


**Fig. 1.** (a) Architecture of the proposed lens elements. The proposed lens elements are mainly composed of a varifocal component and a scanning component. The two components are both driven by the DE actuators. The varifocal component is mainly composed of four acrylic frames, two lens elements of the Alvarez lenses, and two DE membranes. The lateral relative movements of the two lens elements can be realized by applying driving voltages to the right and left compliant electrodes on the DE membrane. Hence, the focal length of the varifocal component can be altered. The DE membrane of the scanning component is divided into four quadrants. The scanning component allows the varifocal component to move in different directions and makes the varifocal component images the region of interest in the center of the field of view by applying voltages on the DE-based four-quadrant actuators. (b) The photograph of the fabricated proposed lens elements with a selectable region of interest capacity using Alvarez lenses actuated by the DE membrane. The magnified picture is the fabricated Alvarez lenses viewed along the optical axis. (c) In the rest state (driving voltage is off), the two lens elements of the Alvarez lenses do not have lateral displacement, and the Alvarez lenses are equivalent to flat plates, i.e., parallel light enters and parallel light exits. (d) In the activation state (driving voltage is on), the focal length of the varifocal component is changed because the two lens elements move relative to each other when an actuation voltage is applied to the DE membrane. The exit light is focused by the varifocal component. (e) The three-dimensional view of the free-form surface of one lens element of the Alvarez lenses.

Similarly, it acts as a concave lens when the first lens element moves in the positive $x$-direction as well as when the second lens element moves in the negative $x$-direction. The focal length of the varifocal component ($f$) can be expressed as

$$f = \frac{1}{4\delta A(n-1)}, \tag{2}$$

where $\delta$ is the lateral displacement, and $n$ is the refractive index of the Alvarez lenses material.

The proposed scanning component is mainly composed of two acrylic frames and one DE membrane. The DE is sandwiched by the two frames. The DE membrane is divided into four quadrants and both sides of the four quadrants are coated with compliant electrodes. These four quadrants are isolated by enough gaps to prevent electrical connection. When the driving voltage is applied to the compliant electrodes of a quadrant, the DE membrane of the actuated quadrant expands in the lateral direction because it is an incompressible material, i.e., its volume does not change. Hence, the varifocal component moves in the lateral direction. By applying actuation voltages to different quadrants, the scanning component allows the varifocal component to move in different directions and makes the varifocal component images the region of interest in the center of the field of view. Therefore, the proposed lens elements can both focus and image the region of interest by applying voltages to the compliant electrodes of the varifocal component and scanning component, respectively.

The fabrication processes of the proposed lens elements are described as follows. First, two lens elements of the Alvarez lenses with a diameter of 6.0 mm are fabricated by a single-point diamond turning technique (Nanoform 250, Precitech) with a programming resolution of 0.01 nm, as shown in the magnified picture in Fig. 1(b). The two lens elements are fabricated from acrylic material with a refractive index of 1.47. The three parameters in Eq. (1), describing the freeform of the two lens elements of the Alvarez lenses are $A = 0.075$ mm$^{-2}$, $D = -0.175$, and $E = 1$ mm, respectively. A MATLAB script is written to present the freeform surface of one lens element of the Alvarez lenses. The three-dimensional view of the free-form surface is illustrated in Fig. 1(e).

Second, the proposed varifocal component can be divided into upper and lower parts. The explosive view of the lower part is shown in Fig. 2(a). Two 2-mm-thick polymethyl methacrylate (PMMA) frames with an inner diameter of 20 mm and an outer diameter of 24 mm are fabricated by a laser engraving machine (4060, Ketailaser Company). The DE membrane (VHB4905, 3M Company) is sandwiched by the two acrylic frames, and the top and bottom sides of the local areas of the DE membrane along the $x$-axis of the Alvarez lenses are coated with carbon powder (BP2000, Carbot) as compliant electrodes. The VHB4905 is biaxially stretched by a factor of 200% to achieve a large strain. Because VHB4905 is a kind of strong adhesion tape, the lens element of the Alvarez lenses and the acrylic frames can directly adhere to the VHB4905. The two

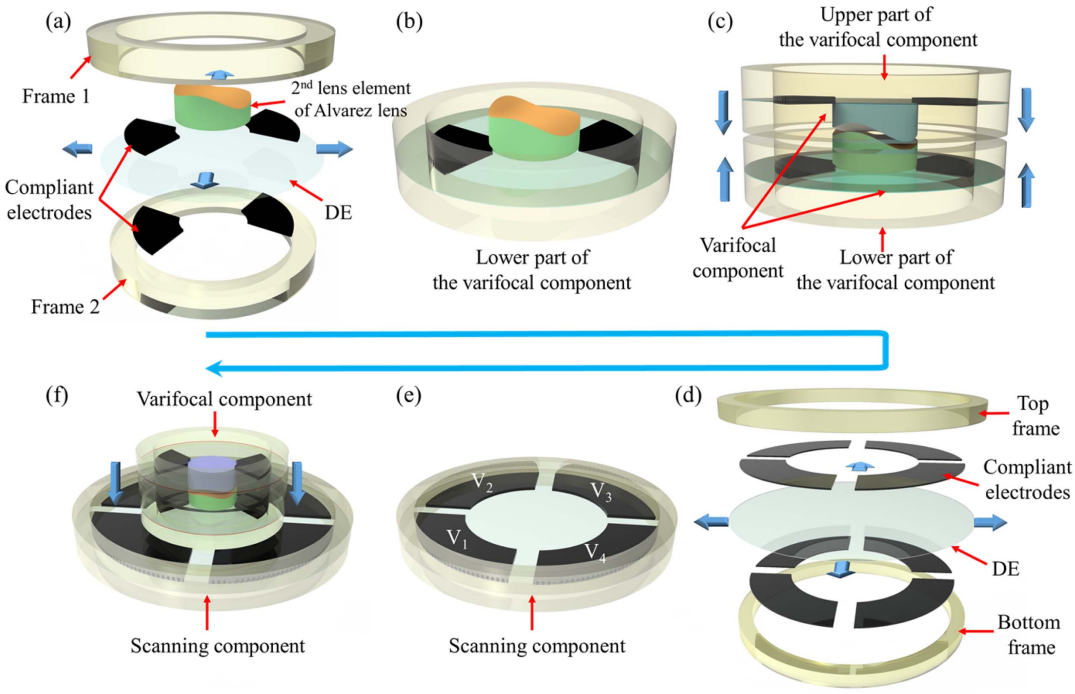


**Fig. 2.** Schematic illustration of the fabrication procedure of the proposed lens elements. (a) The main components of the lower part of the varifocal component. The DE membrane (VHB4905, 3M Company) is pre-stretched with a ratio of 200%. The top and bottom sides of two local areas of the VHB4905 along the *x*-axis are coated with carbon powder (BP2000, Carbot) as compliant electrodes. (b) The assembled lower part of the varifocal component. (c) The upper part of the varifocal component is the same as the lower part, and it is rotated 180° to form the varifocal component together with the lower part. (d) The main components of the scanning component. The DE membrane (VHB4905, 3M Company) is also pre-stretched with a ratio of 200%. The stretched VHB4905 of the scanning component is divided into four quadrants. The four quadrants are coated with carbon powder (BP2000, Carbot) as compliant electrodes on both the top side and the bottom side. (e) The assembled scanning component. (f) The varifocal component is directly attached to the center of the DE membrane of the scanning component due to the inherent strong adhesion of the VHB4905. The whole dimension of the proposed lens elements is 24 mm × 24 mm × 9 mm ($L \times W \times H$).

lens elements of the Alvarez lenses are precisely mounted on the center of the stretched VHB4905 under a microscope camera (GP-530H, Kunshan Gaopin Precision Instrument Company). These components are precisely assembled to form the lower part of the varifocal component, as shown in Fig. 2(b). The fabrication process of the upper part is the same as that of the lower part. Next, the upper part is rotated 180° and is combined with the lower part to form the proposed varifocal component, as shown in Fig. 2(c). It is worth noting that the two lens elements of the Alvarez lenses are separated with an air gap of 300 μm.

Third, the composition of the scanning component is shown in Fig. 2(d). It is mainly composed of two annular acrylic frames (top frame and bottom frame) and one DE membrane with four quadrants ($V_1 - V_4$). The two 1-mm-thick frames have an inner diameter of 40 mm and an outer diameter of 48 mm. With the help of self-designed fan-shaped masks, the carbon powder is printed on the four quadrants of the DE membrane by using a brush. The 56-μm-thick DE membrane of the scanning component is also made from a biaxially stretched VHB4905 by a factor of 200%. The two acrylic frames are adhered to the bottom and top surfaces of the DE membrane, respectively. These components are also subsequently assembled to form the proposed scanning component, as shown in Fig. 2(e). Finally, the varifocal component is directly attached to the center of the stretched VHB4905 of the scanning component. The whole dimension of the proposed lens elements is 24 mm × 24 mm × 9 mm ($L \times W \times H$), as shown in Fig. 2(f).

## 3. EXPERIMENTS AND RESULTS

According to Eq. (2), when the two parameters ($A$ and $n$) of the Alvarez lenses are determined, the focal length of the Alvarez lenses is closely related to the parameter of the lateral displacement ($\delta$). We therefore first measure the lateral displacement of the lens element of the Alvarez lenses by applying different voltages to the compliant electrodes of the DE membrane of the varifocal component. The assembled varifocal component is calibrated under an optical microscope. The lens element can be moved in different directions when applying driving voltages to the different compliant electrodes. When the left compliant electrode is active and the right compliant electrode is inactive, the lens element moves in the right direction. In contrast, when the right compliant electrode is active and the left compliant electrode is inactive, the lens element moves in the left direction. The driving voltage is generated from a voltage-stabilized source (UTP3315TFL-II, UNI-T Company) and is amplified 1200 times by a high voltage converter (A60P-5, XPPOWER Company). The relationship between the lateral displacement

of the lens element of the Alvarez lenses and the driving voltage applied to the active compliant electrode is given in Fig. 3(a). The results reveal that the DE actuator can provide a bi-directional lateral displacement up to ±1.145 mm under a driving voltage of 5.0 kV. Given the lateral displacement ($\delta = 1.145$ mm) and the amplitude coefficient ($A = 0.075$ mm$^{-2}$) as well as the refractive index of the lens material ($n = 1.49$), it is expected that the varifocal component can be tuned from a diverging lens to a converging lens with a theoretical focal length tuning range from $-\infty$ to −5.96 mm and from $+\infty$ to 5.96 mm, according to Eq. (2).

The range of focal length is an important parameter for evaluating the varifocal lens. To qualitatively assess the focal length of the varifocal component based on the Alvarez lenses, the range of the focal length is measured by using the magnification method. A young embryo of a *Capsella bursa-pastoris* section is selected as the imaging object and placed 2.0 mm ($D$) from the varifocal component. By measuring the object height in the captured image under different driving voltages using a microscope, the focal length of the varifocal component is obtained (see Visualization 1). The driving voltage, generated from the voltage-stabilized source and amplified 1200 times by the high voltage converter, is applied to the compliant electrodes through copper foils. The focal length ($f$) is calculated by the following equation, i.e., $f = DM/(M - 1)$, where $M$ is the optical magnification of the object [4]. The focal length of the varifocal component is obtained by both experimental meaurement using the magnification method and theoretical analyses according to Eq. (2). The results are shown in Fig. 3(b), and it shows that the focal lengths obtained by the two methods are in good agreement. From Fig. 3(b), we can also find that the focal length decreases from 181 mm to 5.94 mm with the increase of the driving voltage from 0.2 kV to 5 kV when the varifocal component acts as a convex lens. Meanwhile, the focal length decreases from −181 mm to −5.94 mm with the increase of the driving voltage from 0.2 kV to 5.0 kV when the varifocal component acts as a concave lens. The focal length variation of the proposed varifocal component is up to 30.5 times (181 mm/5.94 mm). The results indicate that the varifocal component can vary its focal length substantially with only a small relative lateral distance between the two lens elements of the Alvarez lenses.

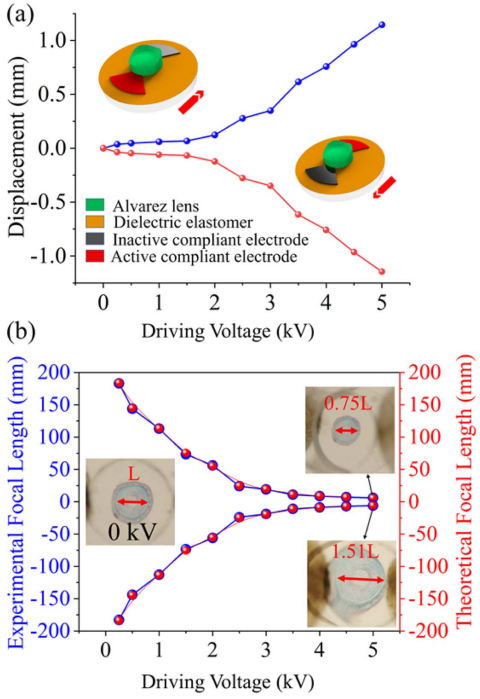


**Fig. 3.** (a) Relationship between the lateral displacement of the lens element of the Alvarez lenses and the driving voltage applied to the active compliant electrode. (b) The experimental and theoretical focal lengths of the varifocal component. The experimental focal length is measured by the magnification method, and the theoretical focal length is evaluated by the lateral displacement according to Eq. (2).

Compared with the traditional varifocal lens, which achieves focusing tuning ability by moving the lens along the optical axis using mechanical parts, the proposed varifocal component tunes the focal length through the lateral displacement of the two lens elements of the Alvarez lenses. Without the movement of any mechanical parts, the proposed varifocal component can focus the objects and obtain clear images at different distances. To qualitatively assess the tunable focal length performance of the proposed varifocal component based on the Alvarez lenses actuated by the DE membrane, images of three objects located at different distances from the varifocal component are obtained by the microscope. The proposed lens elements are mounted at a fixed distance of 3.0 mm from the microscope, and the driving voltage is adjusted until the sharpest image of each object is obtained. The experimental setup and captured images are shown in Fig. 4. Three 1-mm-thick vitreous tissue sections, including the daphnia section, the fibrous connective section, and the young embryo of a *Capsella bursa-pastos* section, are placed before the proposed lens elements with the distances of 3.0 mm, 4.5 mm, and 6.0 mm, respectively. At the driving voltage of 0 kV, the initial focal length of the proposed lens elements makes the daphnia tissue section (Tissue section 1) well focused, and the other two tissue sections are blurred. When the driving voltage is changed to 2.5 kV, the varifocal component focuses on the section of the fibrous connective tissue (Tissue section 2). When the driving voltage increases to 3.6 kV, the young embryo of *Capsella bursa-pastoris* tissue section (Tissue section 3) becomes focused, and the other two sections become blurred. The results show that the proposed lens elements successfully distinguish the objects placed at different distances by changing the actuation voltage (see Visualization 2).

The tuning speed of the focal length is an important parameter for evaluating the dynamic performance of the proposed lens elements. Fast-changing focal length ability is significant for many application scenarios, such as biological cell tracking, smartphones, and aerospace [42,43]. We test the response time of the dynamic performance of the proposed varifocal component. The experimental schematic is shown in Fig. 4(b). A laser light beam is generated by a laser (MGL-III-532, Changchun New Industries Optoelectronics Technology Company) and collimated by a beam expander (GCO02501, Daheng Optics). The collimated beam passes through a diaphragm with a 5-μm-pinhole (GCT-060201, Daheng Optics) and

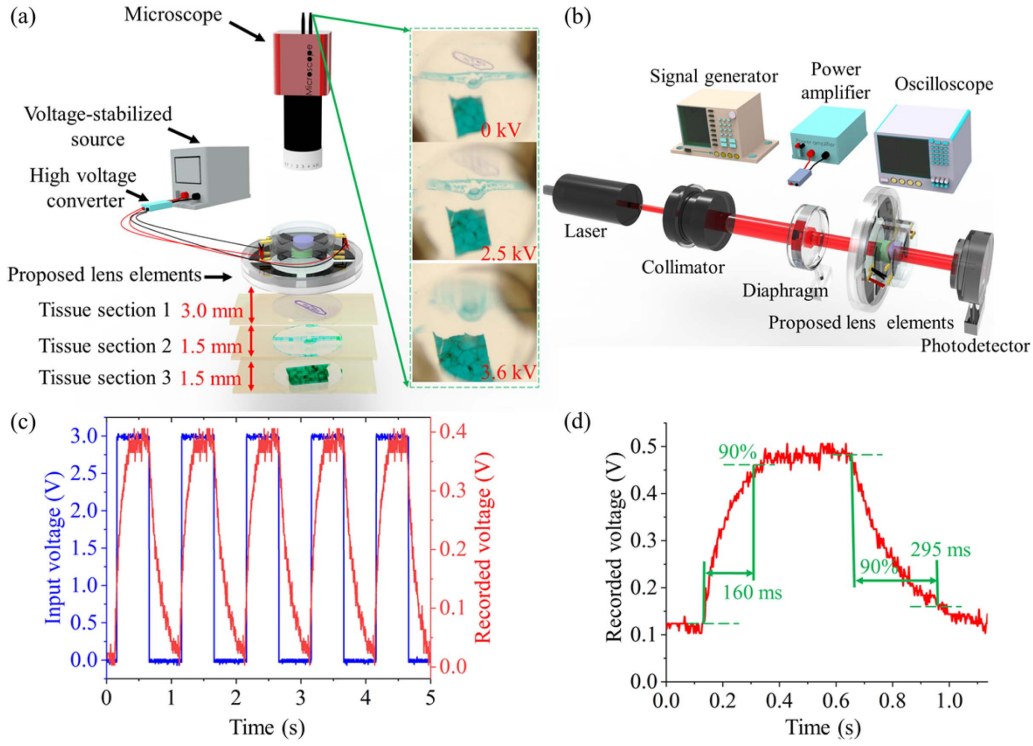


**Fig. 4.** (a) Demonstration of adaptive focusing by viewing three tissue sections placed at different distances from the proposed lens elements. Three tissue sections, including the daphnia (Tissue section 1), the fibrous connective (Tissue section 2), and the young embryo of *Capsella bursa-pastos* (Tissue section 3), are placed before the proposed lens elements with the distances of 3.0 mm, 4.5 mm, and 6.0 mm, respectively. (b) The experimental schematic to test the dynamic response time of the proposed varifocal component. (c) The recorded voltage of the photodetector when the input voltage is a square signal with the frequency of 1 Hz and an amplitude of 3.0 V. (d) The measured rise time and fall time of the proposed varifocal component. The rise and fall times are 160 ms and 295 ms, respectively.

focuses on the photodetector (PDA36A-EC, Thorlabs) through the proposed varifocal component. The photodetector is used to record the light intensity of the laser beam passing through the pinhole. The focal length can be tuned when a driving voltage is applied to the compliant electrode of the DE membrane, which makes the recorded light intensity change and then the recorded voltage different. The dynamic response, when the input voltage generated from the function generator (DG1062, RIGOL Technologies) is a square signal with a frequency of 1 Hz, an amplitude of 3.0 V, and a duty cycle of 50%, is shown in Fig. 4(c). The input voltage is amplified by a power amplifier (PA1011, RIGOL Technologies) and then is applied to the compliant electrode of the DE membrane. The response time of the proposed adaptive lens is obtained from the local magnified area in Fig. 4(c). The rise and fall times are regarded as the time consumption from the initially recorded voltage to 90% of the maximum recorded voltage and from the maximum recorded voltage to 90% of the initially recorded voltage [44], respectively, as shown in Fig. 4(d). We can observe that rise and fall times of the proposed ultra-varifocal component are 160 ms and 295 ms, respectively. Because the DE used for the scanning component has the same stretch ratio as the varifocal component, the response time of the scanning component is in the same order of magnitude as the varifocal component. There are several feasible ways to increase the response speed, including reducing the mass of the two lens elements of the Alvarez lens and using the DE membrane with high stiffness and a high dielectric permittivity.

When the interesting region is not in the center of the field of view of the imaging system, it is necessary to align the central field of view with the region of interest because of the observation habit of the human eye and the high imaging quality in the central field of view. To verify the selectable region of interest capacity, an experimental imaging system based on the proposed lens elements is built to realize ultra-wide varifocal imaging with a selectable region of interest, as shown in Fig. 5(a). A biological intestine tissue section is located at fixed distances of 3.0 mm from the proposed varifocal lens element and is imaged on the microscope through the proposed varifocal lens element. By applying driving voltages to four-quadrant actuators, the scanning component allows the varifocal component to move in different directions and endows the varifocal component with the capacity of making the selectable region of interest in the center of the field of view. At the initial state, there is no driving voltage applied to any quadrants of the scanning component and the varifocal component, and the image is shown in Fig. 5(c). To scan the imaging area and change the focal length, a driving voltage of 4.0 kV generated from the voltage-stabilized source 2 is applied to the varifocal component, and a driving voltage of 5.0 kV generated from the voltage-stabilized source 1 is applied to different quadrants ($V_1$ – $V_4$) of the scanning component. The images are shown

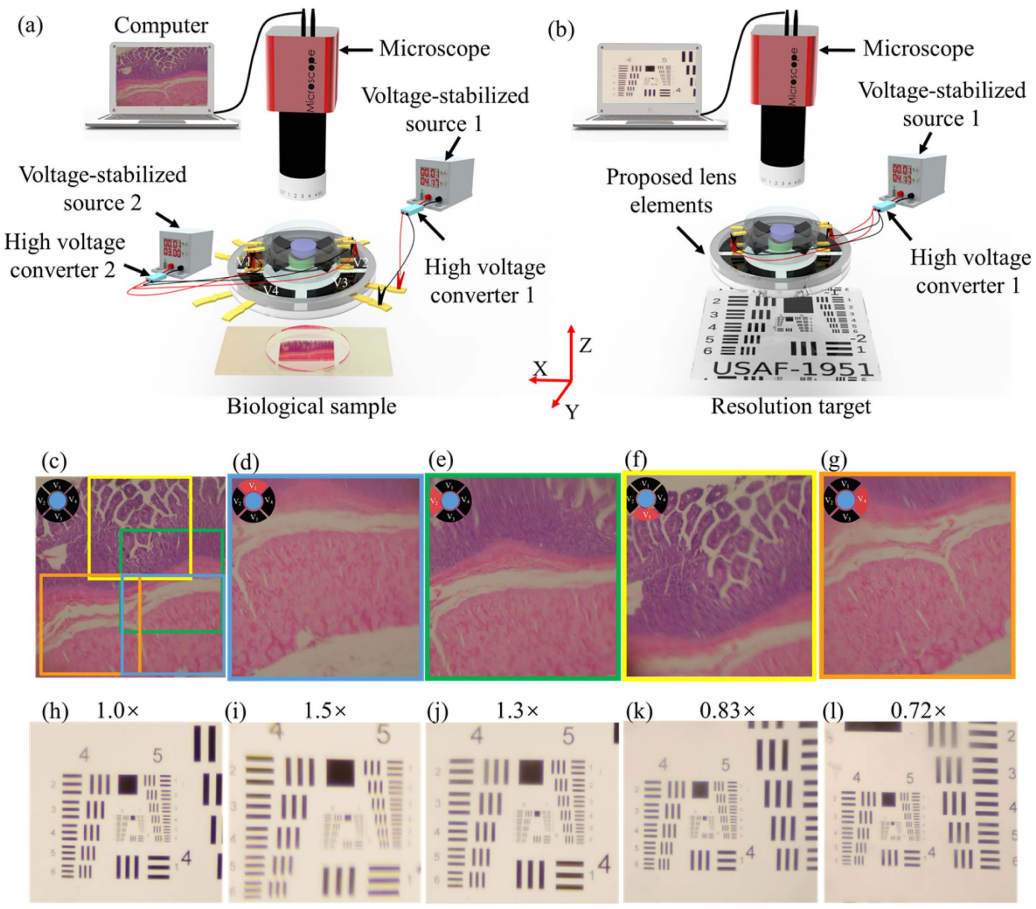


**Fig. 5.** (a) Experimental schematic for evaluating the selectable region of interest capacity of the ultra-wide varifocal imaging system based on the proposed lens elements. By applying actuation voltage on the varifocal component using voltage-stabilized source 2 while applying actuation voltage on the scanning component using voltage-stabilized source 1, the varifocal component can magnify the object, and the scanning component allows the varifocal component to move in different directions, which endows the varifocal component with the capacity of making the selectable region of interest in the center of the field of view. (b) The experimental schematic for characterizing the image resolution of the ultra-wide varifocal imaging system. (c) The image at the rest state. There is no driving voltage applied to any quadrants of the scanning component and the varifocal component. (d)–(g) Images at different actuation states when different driving voltages are applied to the four-quadrant actuators of the scanning component. (h) The image of the resolution target at the rest state. There is no driving voltage applied to the varifocal component. (i)–(l) The images of the resolution target at different actuation states.

in Figs. 5(c)–5(g) (see Visualization 3). When only quadrant 1 ($V_1$) is subjected to a driving voltage generated from voltage-stabilized source 1, the varifocal component moves in the down direction, which makes the center of the imaging field of view located on the down area compared to the initial image. The image when only quadrant 1 is subjected to a driving voltage is shown in Fig. 5(d). The moving distance of the varifocal component is approximately 0.95 mm when the actuation voltage is 5.0 kV. Therefore, we can easily obtain that the scanning range of the scanning component is 17.57° according to the triangle relationship. Similarly, when only quadrant 2 ($V_2$), quadrant 3 ($V_3$), and quadrant 4 ($V_4$) of the scanning component are subjected to a driving voltage of 5.0 kV, the varifocal component moves to the right, up, and left directions, and the images are shown in Figs. 5(e)–5(g), respectively. The results show that the proposed lens elements have the selectable region of interest capacity by applying driving voltages to four-quadrant actuators.

To characterize the image resolution of the ultra-wide varifocal imaging system with a selectable region of interest, a USAF negative resolution target (USAF1951, Edmund Optics) is located at a fixed distance of 3.0 mm from the imaging system, and the image is captured by the microscope through the proposed lens elements. The experimental setup is shown in Fig. 5(b). At the initial state, when there is no driving voltage applied to the varifocal component, the image is shown in Fig. 5(h). Figure 5(h) shows that the proposed lens elements could resolve group 7 and element 1, and the corresponding imaging resolution is approximately 128 lp/mm. When driving voltages of 4.0 kV and 3.0 kV are applied to actuate the first lens element of the Alvarez lenses when it moves along the positive $x$ direction and the second lens element of the Alvarez lenses when it moves along the negative $x$ direction, the varifocal component acts as a convex lens, and the images are magnified by 1.5× and 1.3×, respectively, as shown in Figs. 5(i) and 5(j). From Fig. 5(i), we can find that the proposed lens

elements can resolve group 7 and element 2, and the corresponding resolution is approximately 144 lp/mm. From Fig. 5(j), we can find that the proposed lens elements can still resolve group 7 and element 4, and the corresponding resolution is approximately 181 lp/mm. Because aberrations would be introduced during lateral displacement, the imaging performance of the Alvarez lens decreases with the increase of the element displacement. The dominant aberrations affecting the imaging resolution of the Alvarez lenses are spherical aberrations, defocus, and coma [31]. From Figs. 5(k) and 5(l) are the images when driving voltages of 3.0 kV and 4.0 kV are applied to actuate the first lens element of the Alvarez lenses when it moves along the negative $x$ direction and the second lens element of the Alvarez lenses when it moves along the positive $x$ direction. The varifocal component acts as a concave lens, and the images are magnified by 0.83× and 0.72×, respectively, as shown in Figs. 5(k) and 5(l). From Figs. 5(k) and 5(l), we can find that the proposed lens elements can still resolve group 7 and element 1 (the corresponding resolution is approximately 128 lp/mm). The resolution of the proposed lens elements working as the convex lens is higher than that of the concave lens when the varifocal component is subject to the same driving voltage.

## 4. CONCLUSIONS

In summary, we develop lens elements with a wide focal length tuning range and selectable region of interest capacity. The focal length variation of the proposed lens elements is up to 30.5 times, where the maximum focal length is 181 mm and the minimum focal length is 5.94 mm. The proposed lens elements are composed of the varifocal component and the scanning component. The actuation of the two components is realized by the DE membrane. The function of the variable focal length is achieved based on the Alvarez lenses. The large deformation generated by the DE actuators permits lateral displacement of the Alvarez lenses up to 1.145 mm. The proposed lens elements can both change the focal length and select the region of interest without mechanical movement. The response time of the varifocal component is tested, and the results show that rise and fall times are 160 ms and 295 ms, respectively. Based on the proposed lens elements, an imaging system is built to realize ultra-wide varifocal imaging with a selectable region of interest. The imaging resolution of the system is approximately 181 lp/mm. The demonstrated lens elements provide a pathway to develop ultra-wide varifocal optical imaging systems while retaining high-resolution and fast response speed by combining lateral displacement characteristics of Alvarez lenses and the large deformation ability of the DE membrane. The proposed lens elements still have some drawbacks, such as high voltage actuation, large aberration, and a narrow field-of-view. Further research, including reduction of the actuation voltage and aberrations, enhancing the field-of-view, and implementing of potential imaging applications, will be conducted.

**Funding.** National Natural Science Foundation of China (91420203, 61605008, 61905014, 51735002).

**Disclosures.** The authors declare no conflicts of interest.

**Data Availability.** Data underlying the results presented in this paper are not publicly available at this time but may be obtained from the authors upon reasonable request.

## REFERENCES

1. L. Dong, A. K. Agarwal, D. J. Beebe, and H. Jiang, "Adaptive liquid microlenses activated by stimuli-responsive hydrogels," Nature **442**, 551–554 (2006).
2. L. Dong, A. K. Agarwal, D. J. Beebe, and H. Jiang, "Variable-focus liquid microlenses and microlens arrays actuated by thermoresponsive hydrogels," Adv. Mater. **19**, 401–405 (2007).
3. S. Colburn, A. Zhan, and A. Majumdar, "Varifocal zoom imaging with large area focal length adjustable metalenses," Optica **5**, 825–831 (2018).
4. J. Lee, Y. Park, and S. K. Chung, "Multifunctional liquid lens for variable focus and aperture," Sens. Actuators A **287**, 177–184 (2019).
5. D. Zhu, C. Li, X. Zeng, and H. Jiang, "Tunable-focus microlens arrays on curved surfaces," Appl. Phys. Lett. **96**, 081111 (2010).
6. E. Arbabi, A. Arbabi, S. M. Kamali, Y. Horie, M. Faraji-Dana, and A. Faraon, "MEMS-tunable dielectric metasurface lens," Nat. Commun. **9**, 812 (2018).
7. L. Wang, T. Hayakawa, and M. Ishikawa, "Dielectric-elastomer-based fabrication method for varifocal microlens array," Opt. Express **25**, 31708–31717 (2017).
8. S. Shian, R. M. Diebold, and D. R. Clarke, "Tunable lenses using transparent dielectric elastomer actuators," Opt. Express **21**, 8669–8676 (2013).
9. Q. Chen, T. Li, Y. Zhu, W. Yu, and X. Zhang, "Dielectrophoresis-actuated in-plane optofluidic lens with tunability of focal length from negative to positive," Opt. Express **26**, 6532–6541 (2018).
10. W. Kim, H. C. Yang, and D. S. Kim, "Wide and fast focus-tunable dielectro-optofluidic lens via pinning of the interface of aqueous and dielectric liquids," Opt. Express **25**, 14697–14705 (2017).
11. L. Li, C. Liu, H. Ren, H. Deng, and Q.-H. Wang, "Annular folded electrowetting liquid lens," Opt. Lett. **40**, 1968–1971 (2015).
12. F. Carpi, G. Frediani, S. Turco, and D. De Rossi, "Bioinspired tunable lens with muscle-like electroactive elastomers," Adv. Funct. Mater. **21**, 4152–4158 (2011).
13. L. MaffliS. Rosset, , M. Ghilardi, F. Carpi, and H. Shea, "Ultrafast all-polymer electrically tunable silicone lenses," Adv. Funct. Mater. **25**, 1656–1665 (2015).
14. J. Li and C.-J. Kim, "Current commercialization status of electrowetting-on-dielectric (EWOD) digital microfluidics," Lab Chip **20**, 1705–1712 (2020).
15. K. Wei, H. Zeng, and Y. Zhao, "Insect-human hybrid eye (IHHE): an adaptive optofluidic lens combining the structural characteristics of insect and human eyes," Lab Chip **14**, 3594–3602 (2014).
16. Y. Cheng, C. Chen, J. Cao, C. Bao, A. Yang, and Q. Hao, "Tunable lens using dielectric elastomer sandwiched by transparent conductive liquid," Opt. Lett. **46**, 4430–4433 (2021).
17. N. Hasan, H. Kim, and C. H. Mastrangelo, "Large aperture tunable-focus liquid lens using shape memory alloy spring," Opt. Express **24**, 13334–13342 (2016).
18. M. B. KumarD. Kang, , J. Jung, H. Park, J. Hahn, M. Choi, J.-H. Bae, H. Kim, and J. Park, "Compact vari-focal augmented reality display based on ultrathin, polarization-insensitive, and adaptive liquid crystal lens," Opt. Laser Eng. **128**, 106006 (2020).
19. H.-C. Lin and Y.-H. Lin, "An electrically tunable-focusing liquid crystal lens with a low voltage and simple electrodes," Opt. Express **20**, 2045–2052 (2012).
20. C.-W. Chiu, Y.-C. Lin, P. C.-P. Chao, and A. Y.-G. Fuh, "Achieving high focusing power for a large-aperture liquid crystal lens with novel hole-and-ring electrodes," Opt. Express **16**, 19277–19284 (2008).
21. Z. Han, S. Colburn, A. Majumdar, and K. F. Böhringer, "Millimeter-scale focal length tuning with MEMS-integrated meta-optics employing high-throughput fabrication," Sci. Rep. **12**, 5385 (2022).
22. W. Zhang, H. Zappe, and A. Seifert, "Polyacrylate membranes for tunable liquid-filled microlenses," Opt. Eng. **52**, 046601 (2013).

23. J. E. M. Whitehead, A. Zhan, S. Colburn, L. Huang, and A. Majumdar, "Fast extended depth of focus meta-optics for varifocal functionality," Photon. Res. **10**, 828–833 (2022).
24. L. Alvarez, "Two-element variable-power spherical lens," U.S. patent US3305294A (21 February 1967).
25. A. W. Lohmann, "A new class of varifocal lenses," Appl. Opt. **9**, 1669–1671 (1970).
26. S. Barbero, "The Alvarez and Lohmann refractive lenses revisited," Opt. Express **17**, 9376–9390 (2009).
27. M. Peloux and L. Berthelot, "Optimization of the optical performance of variable-power and astigmatism Alvarez lenses," Appl. Opt. **53**, 6670–6681 (2014).
28. A. Wilson and H. Hua, "Design and demonstration of a vari-focal optical see-through head-mounted display using freeform Alvarez lenses," Opt. Express **27**, 15627–15637 (2019).
29. Y. Zou, W. Zhang, F. Tian, F. S. Chau, and G. Zhou, "Development of miniature tunable multi-element Alvarez lenses," IEEE J. Sel. Top. Quantum Electron. **21**, 100–107 (2015).
30. Z. Han, S. Colburn, A. Majumdar, and K. F. Böhringer, "MEMS-actuated metasurface Alvarez lens," Microsyst. Nanoeng. **6**, 79 (2020).
31. Y. Zou, G. Zhou, Y. Du, and F. S. Chau, "Alignment tolerances and optimal design of MEMS-driven Alvarez lenses," J. Opt. **15**, 125711 (2013).
32. G. Zhou, H. Yu, and F. S. Chau, "Microelectromechanically-driven miniature adaptive Alvarez lens," Opt. Express **21**, 1226–1233 (2013).
33. S. Petsch, A. Grewe, L. Köbele, S. Sinzinger, and H. Zappe, "Ultrathin Alvarez lens system actuated by artificial muscles," Appl. Opt. **55**, 2718–2723 (2016).
34. Y. Zou, W. Zhang, F. S. Chau, and G. Zhou, "Miniature adjustable-focus endoscope with a solid electrically tunable lens," Opt. Express **23**, 20582–20592 (2015).
35. Y. Zou, F. S. Chau, and G. Zhou, "Ultra-compact optical zoom endoscope using solid tunable lenses," Opt. Express **25**, 20675–20688 (2017).
36. J. Li, Y. Wang, L. Liu, S. Xu, Y. Liu, J. Leng, and S. Cai, "A biomimetic soft lens controlled by electrooculographic signal," Adv. Funct. Mater. **29**, 1903762 (2019).
37. C. Guo, S. Jiang, L. Yang, P. Song, T. Wang, X. Shao, Z. Zhang, M. Murphy, and G. Zheng, "Deep learning-enabled whole slide imaging (DeepWSI): oil-immersion quality using dry objectives, longer depth of field, higher system throughput, and better functionality," Opt. Express **29**, 39669–39684 (2021).
38. S. Nam, S. Yun, J. W. Yoon, S. Park, S. K. Park, S. Mun, B. Park, and K. U. Kyung, "A robust soft lens for tunable camera application using dielectric elastomer actuators," Soft Robot **5**, 777–782 (2018).
39. G. Li, X. Chen, F. Zhou, Y. Liang, Y. Xiao, X. Cao, Z. Zhang, M. Zhang, B. Wu, S. Yin, Y. Xu, H. Fan, Z. Chen, W. Song, W. Yang, B. Pan, J. Hou, W. Zou, S. He, X. Yang, G. Mao, Z. Jia, H. Zhou, T. Li, S. Qu, Z. Xu, Z. Huang, Y. Luo, T. Xie, J. Gu, S. Zhu, and W. Yang, "Self-powered soft robot in the Mariana trench," Nature **591**, 66–71 (2021).
40. A. She, S. Zhang, S. Shian, D. R. Clarke, and F. Capasso, "Adaptive metalenses with simultaneous electrical control of focal length, astigmatism, and shift," Sci. Adv. **4**, 9957 (2018).
41. L. W. Alvarez and W. E. Humphrey, "Variable-power lens and system," US patent US3507565A (21 April 1970).
42. M. Bawart, A. Jesacher, P. Zelger, S. Bernet, and M. Ritsch-Marte, "Modified Alvarez lens for high-speed focusing," Opt. Express **25**, 29847–29855 (2017).
43. S. Y. Kang, M. Duocastella, and C. B. Arnold, "Variable optical elements for fast focus control," Nat. Photonics **14**, 533–542 (2020).
44. H. Ren and S.-T. Wu, "Adaptive lenses based on soft electroactive materials," Appl. Sci. **8**, 1085 (2018).